Supporting Information

Dynamic time-warping correction for shifts in ultrahigh resolving power ion mobility spectrometry and structures for lossless ion manipulations (SLIM)

Adam L. Hollerbach[1], Christopher R. Conant[1], Gabe Nagy[1], Matthew Monroe[1], Khushboo Gupta[1], Micah Donor[1], Cameron M. Giberson[1], Sandilya V. B. Garimella[1], Richard D. Smith[*1], and Yehia M. Ibrahim[*1]

[1] Biological Sciences Division, Pacific Northwest National Laboratory, P.O. Box 999, Richland, Washington, 99354, United States

Corresponding Authors

* rds@pnnl.gov, yehia.ibrahim@pnnl.gov

Table of Contents

Table S1: List of components in a phosphopeptide mixture S3
Table S2: Table of peak measurements for negative Agilent tuning mixture ions S4
Additional description of dynamic time warping S5
Figure S1: DTW applied to a mobility spectrum possessing 10,000 data points and 3 peaks S6
Figure S2: Pressure shifts and Agilent tuning mixture ion responses when opening and closing the ion source housing S7
Figure S3: DTW applied to the 1st separation of negative Agilent tuning mixture ions during opening and closing of the ion source housing S8
Figure S4: DTW applied to the 25th separation of negative Agilent tuning mixture ions during opening and closing of the ion source housing S9
Figure S5: DTW applied to the 50th separation of negative Agilent tuning mixture ions during opening and closing of the ion source housing S10
Description of mobility shifts due to large pressure fluctuations S11
Figure S6: Unaligned and aligned mobility spectra of negative Agilent tuning mixture ions with large arrival time shifts S12
Figure S7: DTW applied to the 1st separation of negative Agilent tuning mixture ions with large arrival time shifts S13
Figure S8: DTW applied to the 25th separation of negative Agilent tuning mixture ions with large arrival time shifts S14
Figure S9: DTW applied to the 50th separation of negative Agilent tuning mixture ions with large arrival time shifts S15
Table S3: Resolving powers using different separation numbers as the reference for DTW S16
Figure S10: DTW applied to the 1st separation of a phosphopeptide mixture S17
Figure S11: DTW applied to the 7th separation of a phosphopeptide mixture S18
Figure S12: DTW applied to the 39th separation of a phosphopeptide mixture S19
Description of SVA and DTW effects on the resolution of phosphopeptide isomers S20
Figure S13: SVA and DTW effects on the resolution of phosphopeptide isomers S21
Figure S14: SVA alignment using different Agilent tuning mixture ions as the reference peak S22
Figure S15: Artifact generation in DTW and parameter adjustments to avoid it S23

Figure S16: Power and linear function fits to a plot of CCS vs arrival time for negative Agilent tuning mixture ions S24
References S25

Table S1: List of components in a phosphopeptide mixture.[1] Y(p), T(p), and S(p) indicate the addition of a phosphate group to tyrosine, threonine, or serine. The asterisk (*) indicates heavy labeling of lysine or arginine.

Peptide Sequences and Modifications	
AVDGY(p)VKPQIK*	RCPT(p)PEIQKK*
AVLPVT(p)CHRDSFSR*	RLS(p)MEIEK*
DS(p)IPQVLLPEEEK*	RNTIDSTS(p)SFSQFR*
ERGSDAS(p)GQLFHGR*	RSDSASS(p)EPVGIYQGFEK*
EYDRLY(p)EEYTR*	S(p)PQMVSAIVR*
GSDAS(p)GQLFHGR*	S(p)VIDTSTIVR*
KDS(p)IPQVLLPEEEK*	SDSASS(p)EPVGIYQGFEK*
KLT(p)LQSAK*	SPS(p)GSAFGSQENLR*
KPS(p)EEEYVIR*	SRT(p)SVQTEDDQLIAGQSAR*
KQISGQYSGS(p)PQLLK*	SS(p)SPELVTHLK*
LDGGRQS(p)TGAVSLK*	SSS(p)PELVTHLK*
LGTGFNPNT(p)LDK*	SYSS(p)PDITQAIQEEEK*
LGTGFNPNT(p)LDKQK*	T(p)SVQTEDDQLIAGQSAR*
LS(p)MEIEK*	TELIS(p)VSEVHPSR*
LT(p)LQSAK*	TPS(p)SEEISPTK*
LY(p)EEYTR*	TPS(p)SEEISPTKFPGLYR*
MNS(p)LTFK*	TPSSEEIS(p)PTK*
MNS(p)LTFKK*	TPSSEEIS(p)PTKFPGLYR*
NTIDSTS(p)SFSQFR*	VDYESQSTDTQNFS(p)SESK*
QISGQYSGS(p)PQLLK*	YLSFT(p)PPEK*
QS(p)TGAVSLK*	YLSFT(p)PPEKDGFPSGTPALNAK*

Table S2: Values for average ATD, standard deviation, max absolute ATD shift, and max percent ATD shift for negative Agilent tuning mixture ions obtained over 50 separations.

m/z	Ave ATD ± 1 Std Dev (ms)	Max Abs Shift (ms)	Max % Shift
1034	503.6 ± 2.3	4.2	0.8
1334	674.4 ± 2.9	4.6	0.7
1634	897.4 ± 3.4	5.5	0.6
1934	1126.5 ± 3.9	6.5	0.6
2234	1336.3 ± 4.9	7.1	0.5
2534	1599.0 ± 5.7	8.4	0.5

Description of DTW applied to data with more points and peaks

Figure S1 shows the DTW process applied to sample and reference ion mobility spectra possessing 10,000 data points and three peaks. Each peak possesses different intensities and widths. The bottom panel of the figure shows the mobility spectrum of the sample (red trace) and reference (light blue) it is being aligned to. The three panels above the mobility spectra correlate to steps D through I from Figure 4. The green line represents the time shifts associated with the smallest Euclidean distances (Figure 4G, green circles), the yellow line represents the smoothed time shifts (Figure 4G, yellow trace), and the red line represents the optimized time shifts after identifying data islands (Figure 4I). The gray regions are meant to guide the eye to important features in the DTW process.

For the following description, the reader is directed to the green line (i.e. Figure S1A). As can be seen, the green line is horizontal for all the data points before the first peak, indicating that these points are all shifted by 0 (i.e. no shifting). Once the first peak is encountered, a vertical line is drawn. This indicates that the data points comprising the top and bottom edges of the vertical line will have different offsets (e.g. 625 versus 0). The vertical line is followed by another horizontal region, indicating a constant shift of about 625 time units for all data points before the second peak. A second vertical line is then drawn when the second peak is encountered, once more indicating a drastic change in the time shifts of adjacent data points. All data points after this second vertical line are then shifted by ~1250 time units, indicated by the horizontal line. A third vertical line is drawn when the third peak is encountered, followed again by a horizontal line that indicates a shift of about 1870 time units for data points after the third peak. The slope of the line then decreases diagonally towards the end of the mobility spectrum. Note that the offset (y-axis) is still positive, meaning that data points corresponding to this diagonal region are still being shifted in the positive time dimension. However, the decreasing slope means that each data point in this region does not shift by as much as the data point preceding it. This phenomenon occurs at the end of mobility spectra because there are no data points beyond what is in the reference spectrum, and DTW does not create extra time points. In other words, the maximum time domain that can be used is determined by the time domain of the reference spectrum. This does mean that any peaks located at the very end of a mobility spectrum will be poorly warped. However, this can be avoided in practice by simply increasing the length of the separation (i.e. more time points at the end).

There are two differences between the green and yellow traces (i.e. Figure S1A and Figure S1B). The first difference is that the green trace is not smooth. This is because the mobility spectra possessed small amounts of noise, and therefore data points can align to noisy areas of peaks. However, it is unlikely that adjacent points will shift by drastically different amounts and smoothing reduces this effect. The second difference is at the locations of the vertical lines. The vertical lines in the green trace are diagonal in the yellow trace. Again, the vertical line indicates that adjacent points will shift by drastically different amounts, which is not likely. However, it is also unlikely that points inside of a peak will shift by differing amounts (in general). The red trace (Figure S1C) shows the time shifts calculated after peak islands are identified. Peak identifications manifest as horizontal lines that are located between two horizontal regions. This step ensures that all data points comprising a peak are shifted by the same amount. An important feature to note is that any data points that do not reside in a peak are shifted by the time shift value calculated in the yellow trace. In other words, the only difference between the red and yellow traces is the red trace incorporates peak islands.

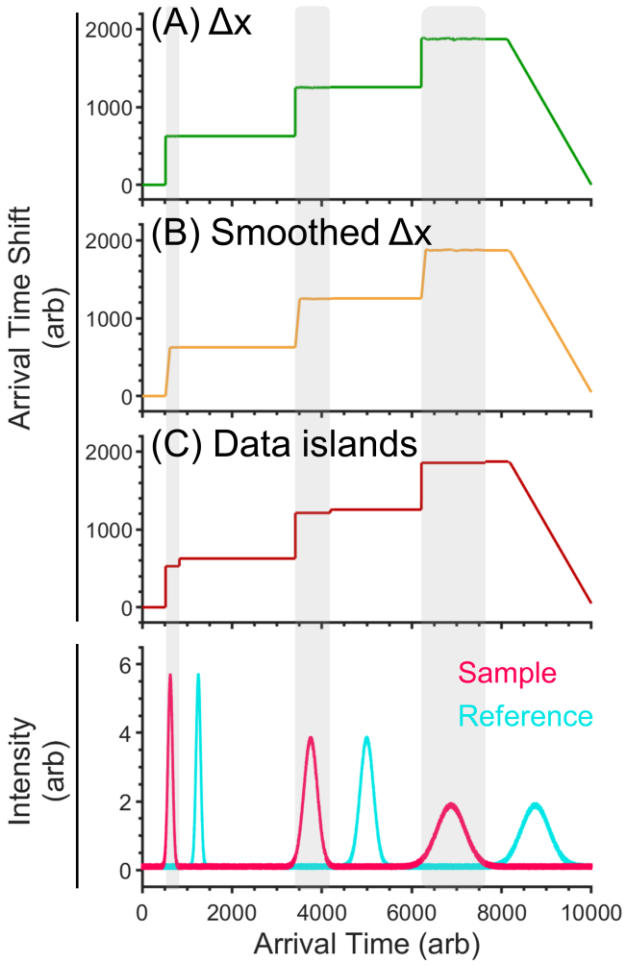

Figure S1: Process of applying dynamic time warping to an artificially generated ion mobility spectrum containing 10,000 data points and 3 peaks. (A) Time shifts, (B) smoothed time shifts, and (C) time shifts after identifying data islands. The bottom panel shows the mobility spectrum of the sample (red trace) and reference (light blue).

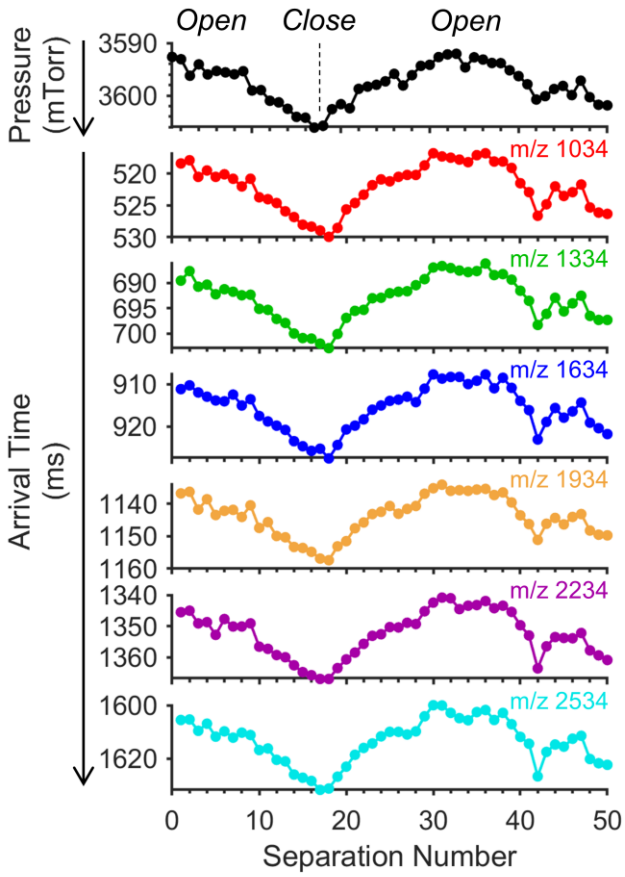

Figure S2: (Black) Pressure shifts measured inside the multilevel SLIM chamber as the ion source housing is opened and closed. Pressure measurements were performed at 10 Hz. Each point represents the average of all pressure measurements performed in a single separation. ATD shifts associated with pressure fluctuations for ions with m/z 1034 (red), 1334 (green), 1634 (blue), 1934 (orange), 2234 (purple), and 2534 (light blue).

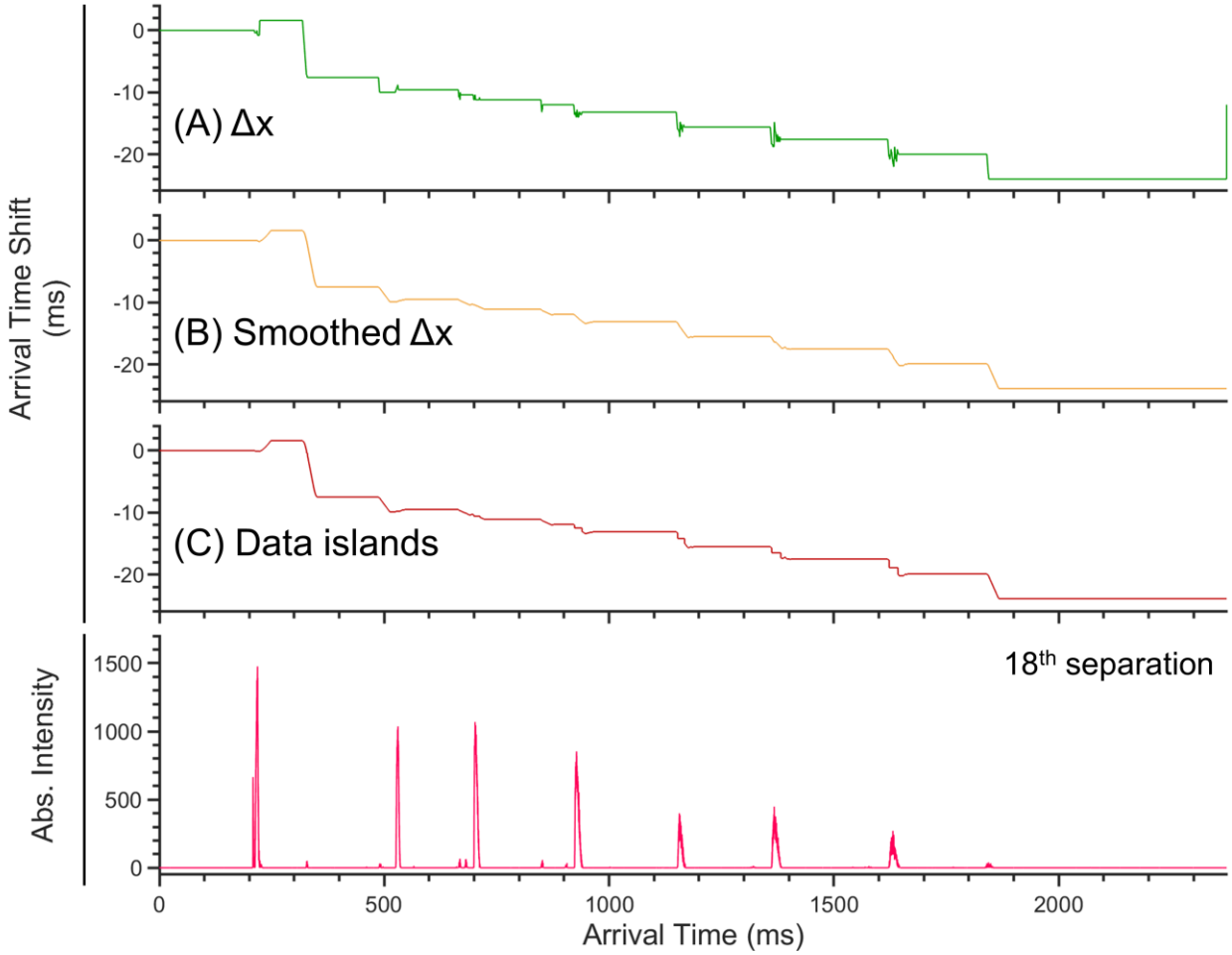

Figure S3: Dynamic time warping process applied to the **18th separation** of negative Agilent tuning mixture ions out of 50 total separations. (A) Arrival time shifts, (B) smoothed arrival time shifts, and (C) arrival time shifts after identifying data islands. Data were acquired during induced pressure fluctuations caused by opening and closing the door to the ion source housing.

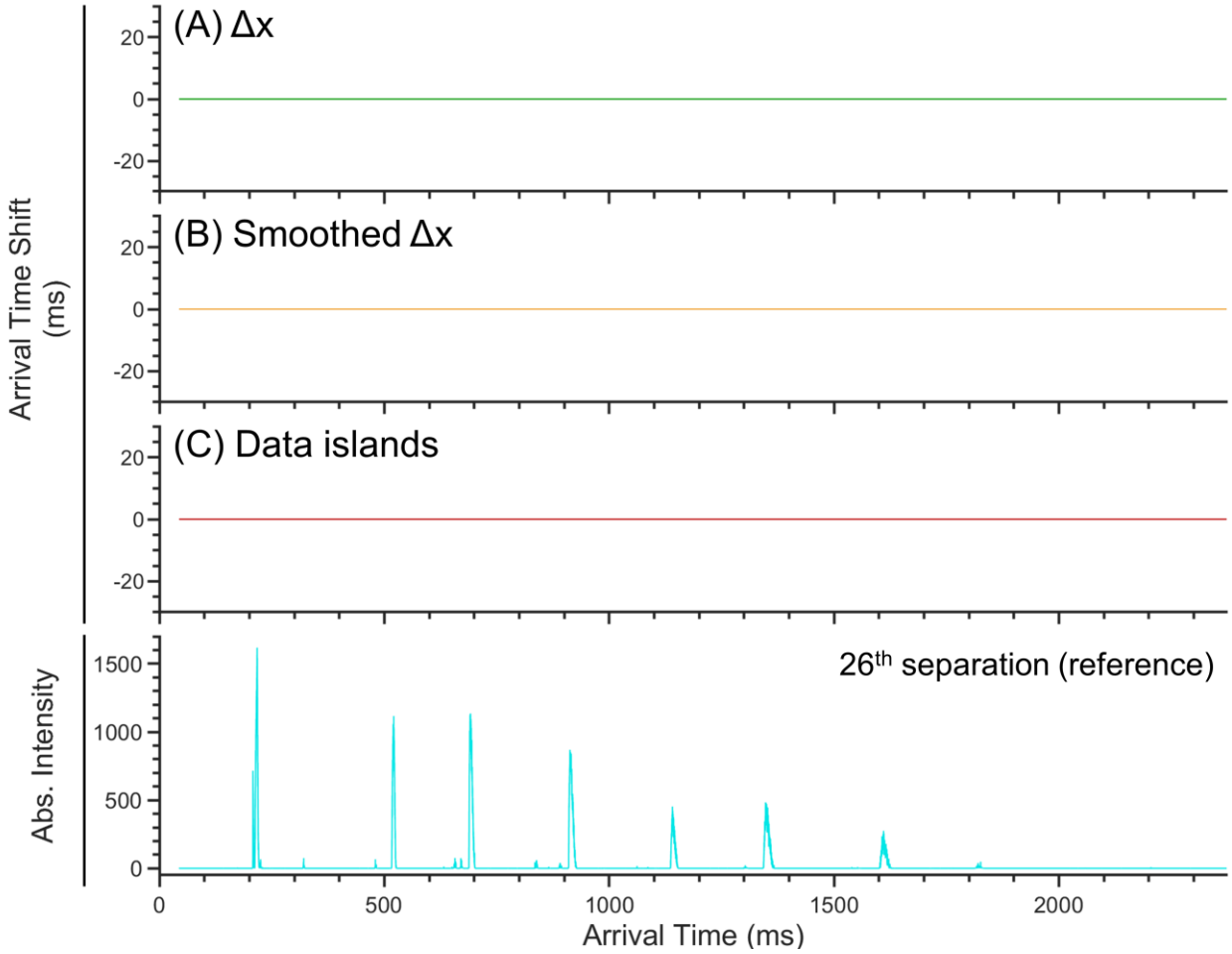

Figure S4: Dynamic time warping process applied to the **26th separation** (reference) of negative Agilent tuning mixture ions out of 50 total separations. (A) Arrival time shifts, (B) smoothed arrival time shifts, and (C) arrival time shifts after identifying data islands. Data were acquired during induced pressure fluctuations caused by opening and closing the door to the ion source housing.

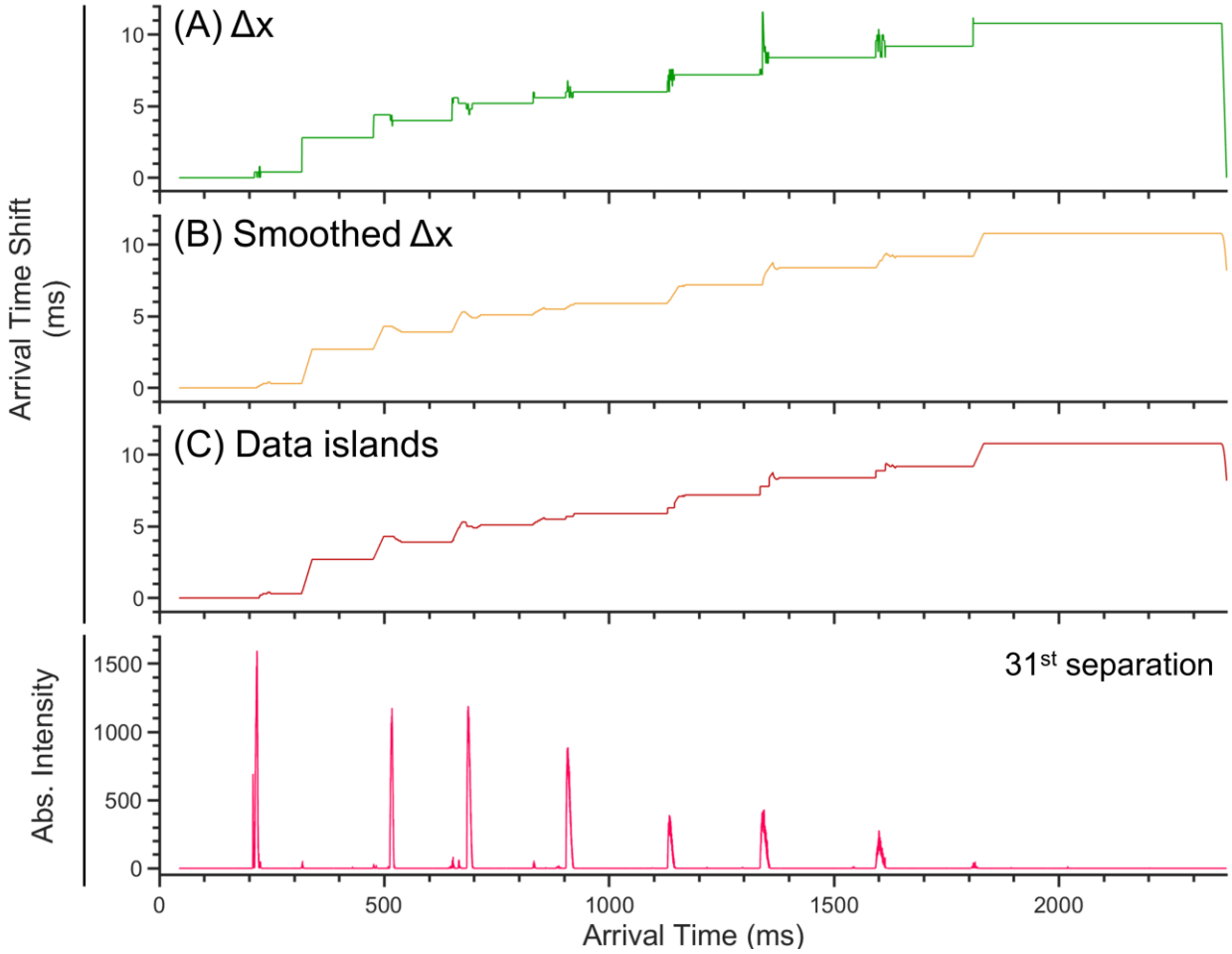

Figure S5: Dynamic time warping process applied to the **31st separation** of negative Agilent tuning mixture ions out of 50 total separations. (A) Arrival time shifts, (B) smoothed arrival time shifts, and (C) arrival time shifts after identifying data islands. Data were acquired during induced pressure fluctuations caused by opening and closing the door to the ion source housing.

Description of mobility spectra possessing large mobility shifts

The red trace in Figure S6A shows the sum of fifty unaligned separations. As can be seen, individual Agilent tuning mixture peaks (m/z 1034-2534) split into three low intensity peaks. The SVA aligner was then applied and each m/z only exhibited one peak (Figure S6A, green trace). However, peak widths were noticeably larger for lower mobility ions (e.g. 2234 & 2534), again illustrating that ions with different mobilities exhibit different absolute mobility shifts in response to instrumental fluctuations in TW-SLIM. The same mobility spectrum was then subject to DTW (Figure S6A, blue trace). Once more, the split peaks in the unaligned data were merged into one peak per m/z in the aligned data. However, the peaks of the lower mobility ions were significantly narrower after DTW, even though both aligners yielded narrow peak widths for higher mobility ions. Rps were calculated for all peaks (Figure S6B). Both aligners yielded Rps of ~82 for m/z 1034 and ~105 for m/z 1334, demonstrating similar performance. However, the SVA aligner yielded an Rp of ~67 for m/z 1934 while the DTW aligner yielded ~120. The discrepancy between Rps worsened as m/z increased (i.e. ion mobility decreased). The SVA aligner yielded Rps of ~53 and ~46 for m/z's 2234 and 2534, respectively, while the DTW aligner yielded ~109 and ~120 for the same m/z's, which are significantly higher.

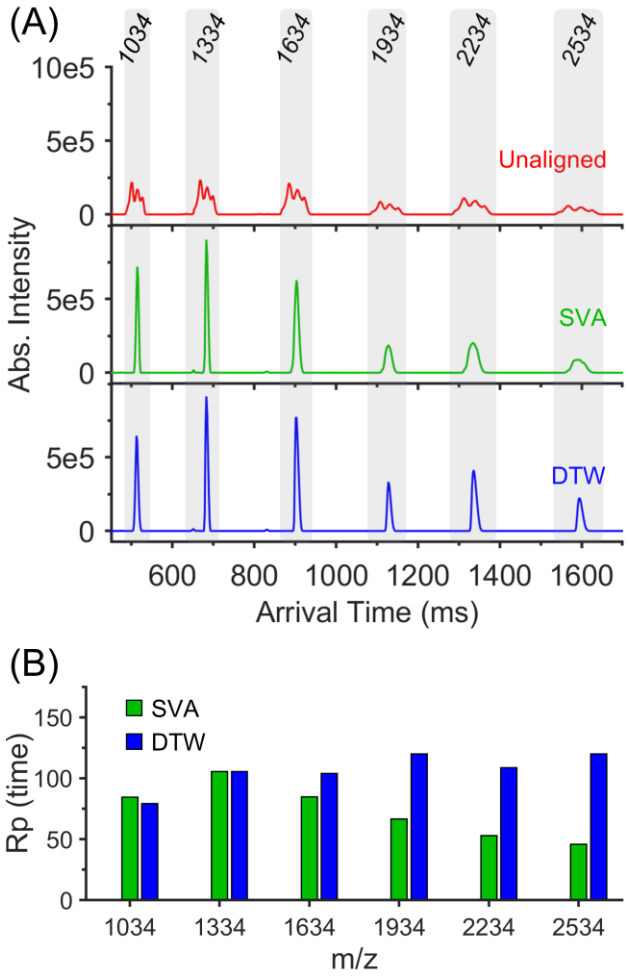

Figure S6: (A) Unaligned (red), SVA (green), and dynamic time warping aligned (blue) mobility spectra of negative Agilent tuning mix ions (m/z 1034, 1334, 1634, 1934, 2234, 2534). Time-based resolving power measurements for negative Agilent tuning mixture ions after SVA (green) and dynamic time warping (blue) alignment. Sum of 50 separations.

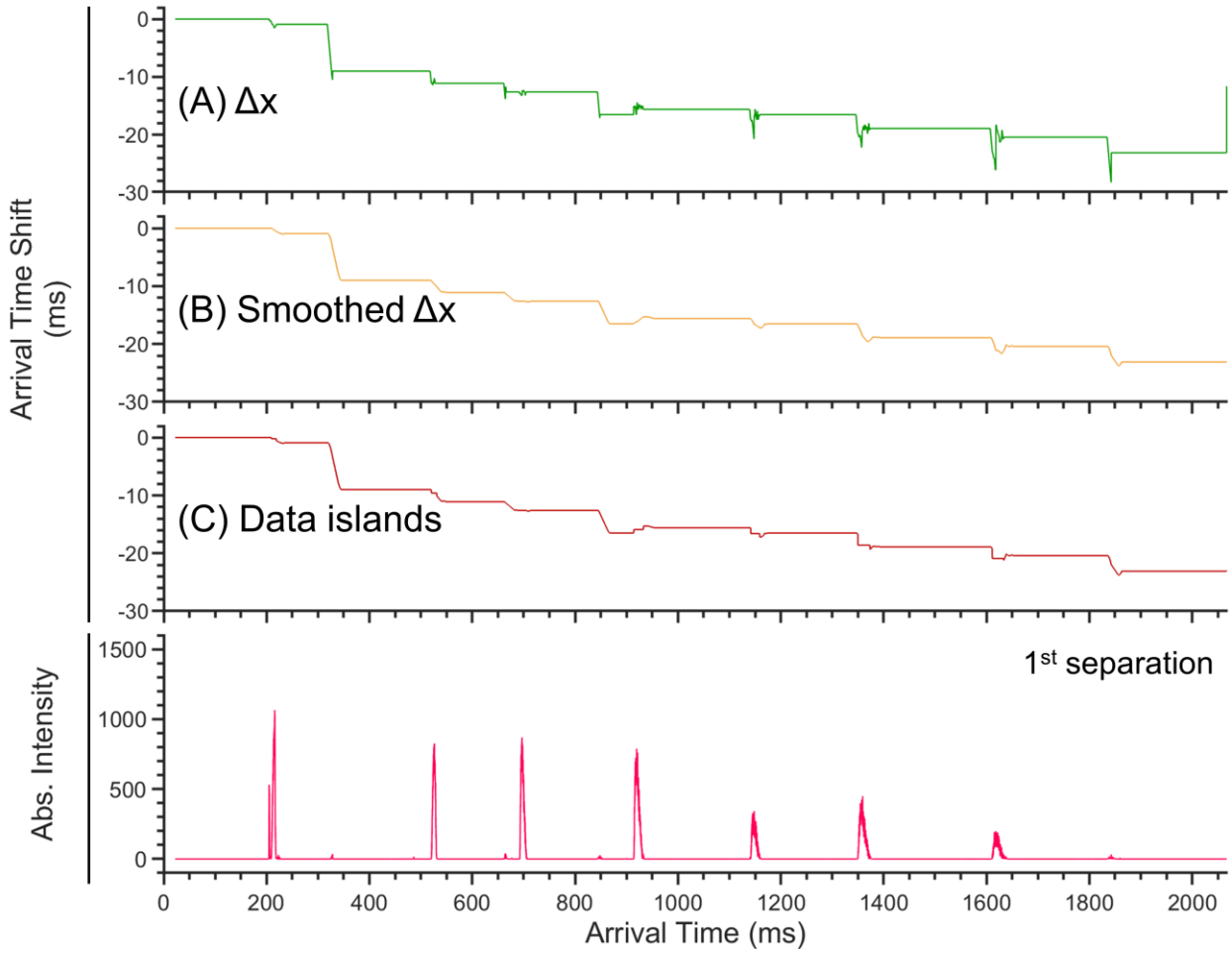

Figure S7: Dynamic time warping process applied to the **1st separation** of negative Agilent tuning mixture ions out of 50 total separations. (A) Arrival time shifts, (B) smoothed arrival time shifts, and (C) arrival time shifts after identifying data islands.

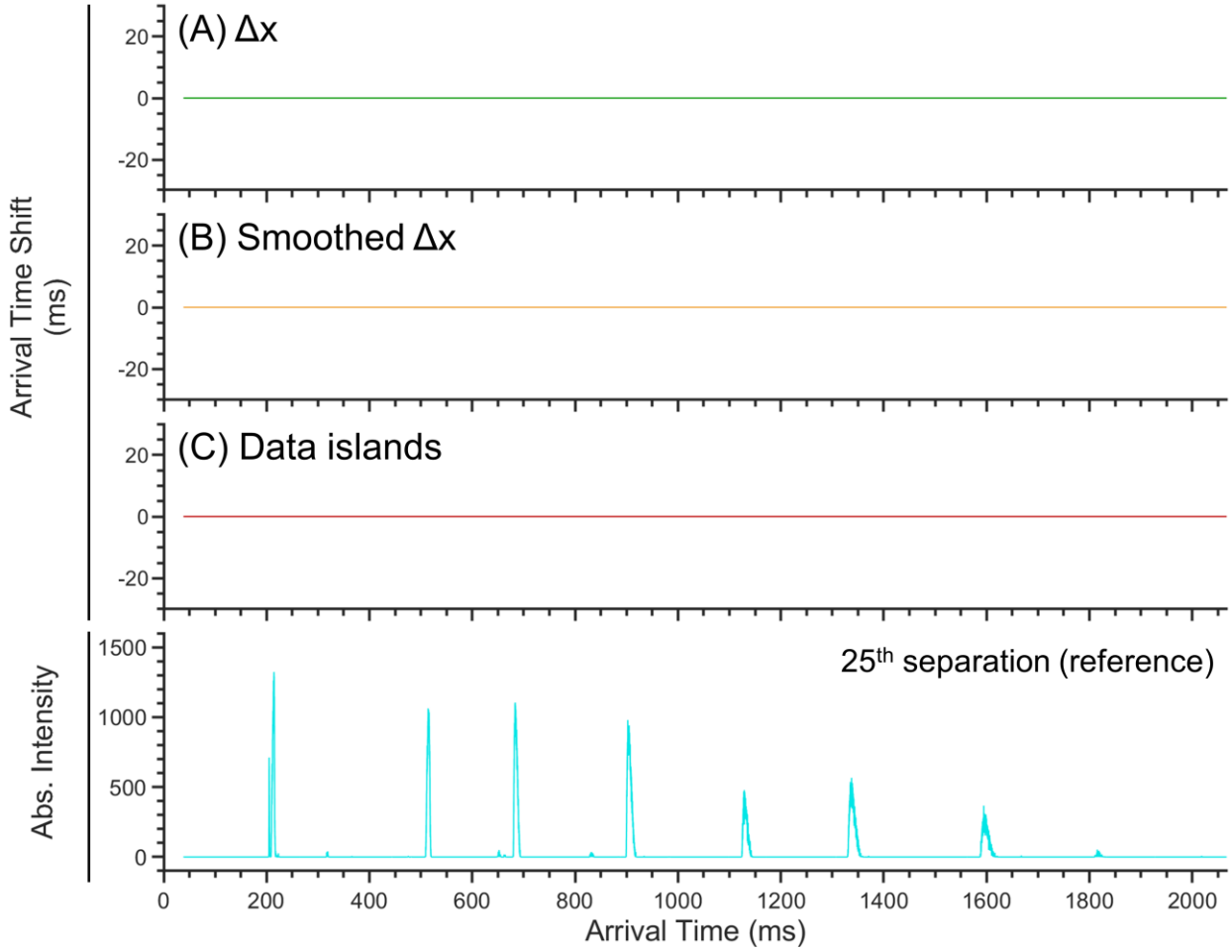

Figure S8: Dynamic time warping process applied to the **25th separation** of negative Agilent tuning mixture ions out of 50 total separations. (A) Arrival time shifts, (B) smoothed arrival time shifts, and (C) arrival time shifts after identifying data islands.

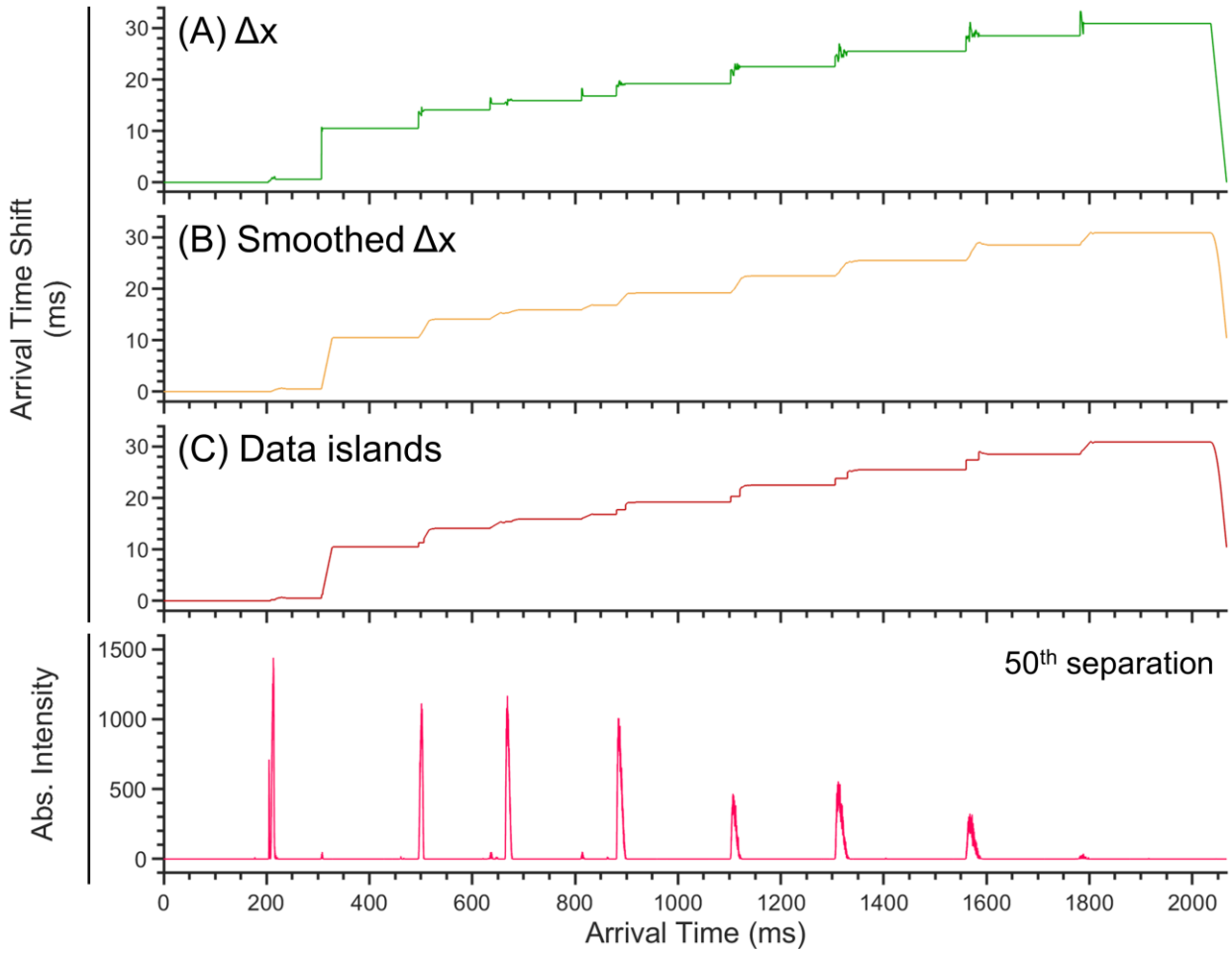

Figure S9: Dynamic time warping process applied to the **50th separation** of negative Agilent tuning mixture ions out of 50 total separations. (A) Arrival time shifts, (B) smoothed arrival time shifts, and (C) arrival time shifts after identifying data islands.

Table S3: Time-based resolving powers calculated for six negative Agilent tuning mixture ions (m/z 1034, 1334, 1634, 1934, 2234, 2534) using different separations as the reference separation for DTW. The total number of separations is 50.

	Resolving power (time)						
	Reference Separation						
m/z	10	20	30	40	50	Ave	Std Dev
1034	84	83	80	97	81	85	7
1334	109	107	105	103	105	106	2
1634	107	105	105	102	103	104	2
1934	125	124	123	121	122	123	1
2234	111	109	109	107	108	109	1
2534	122	120	120	117	118	120	2

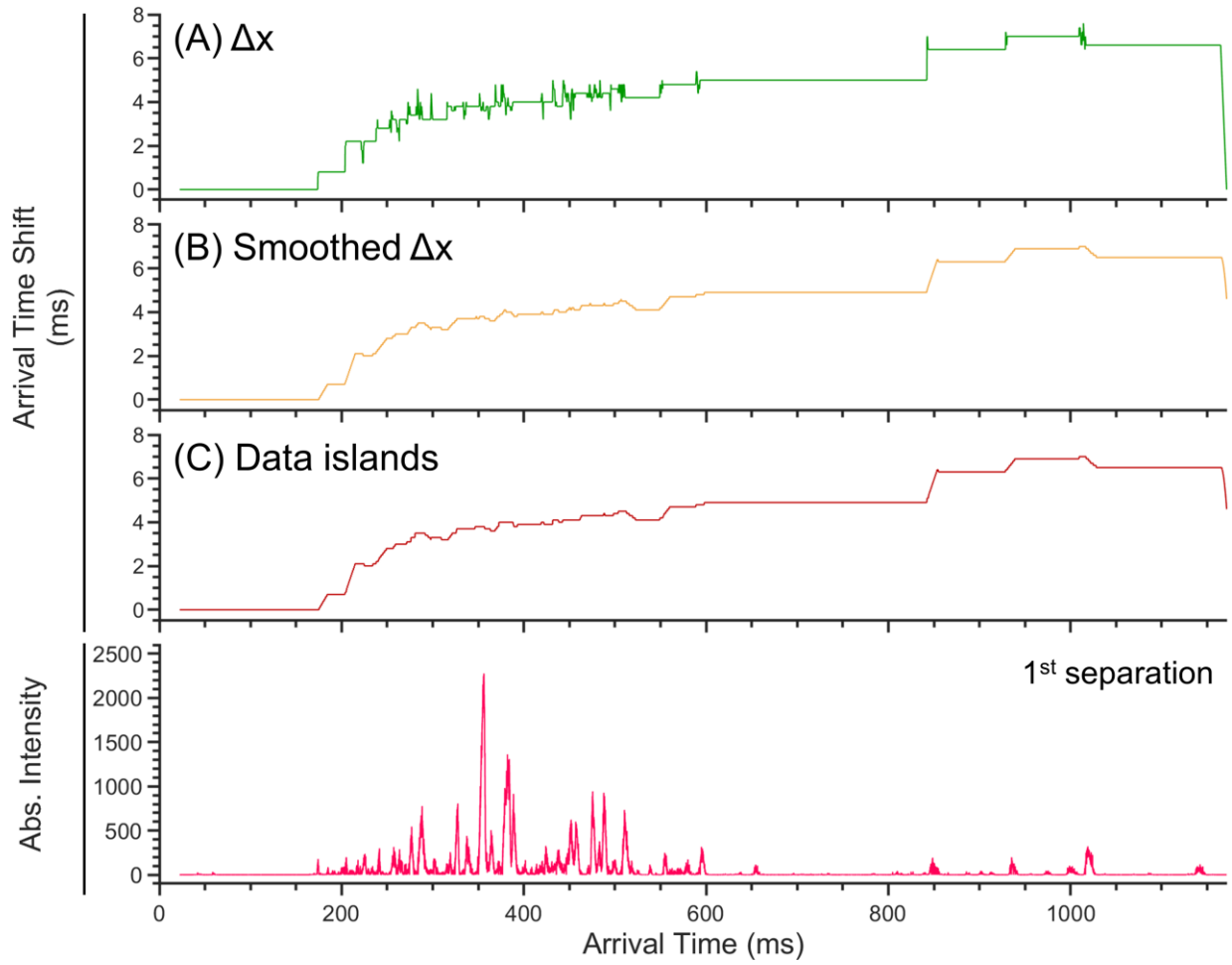

Figure S10: Dynamic time warping process applied to the **1st separation** of ions in a phosphopeptide mixture out of 100 total separations. (A) Arrival time shifts, (B) smoothed arrival time shifts, and (C) arrival time shifts after identifying data islands.

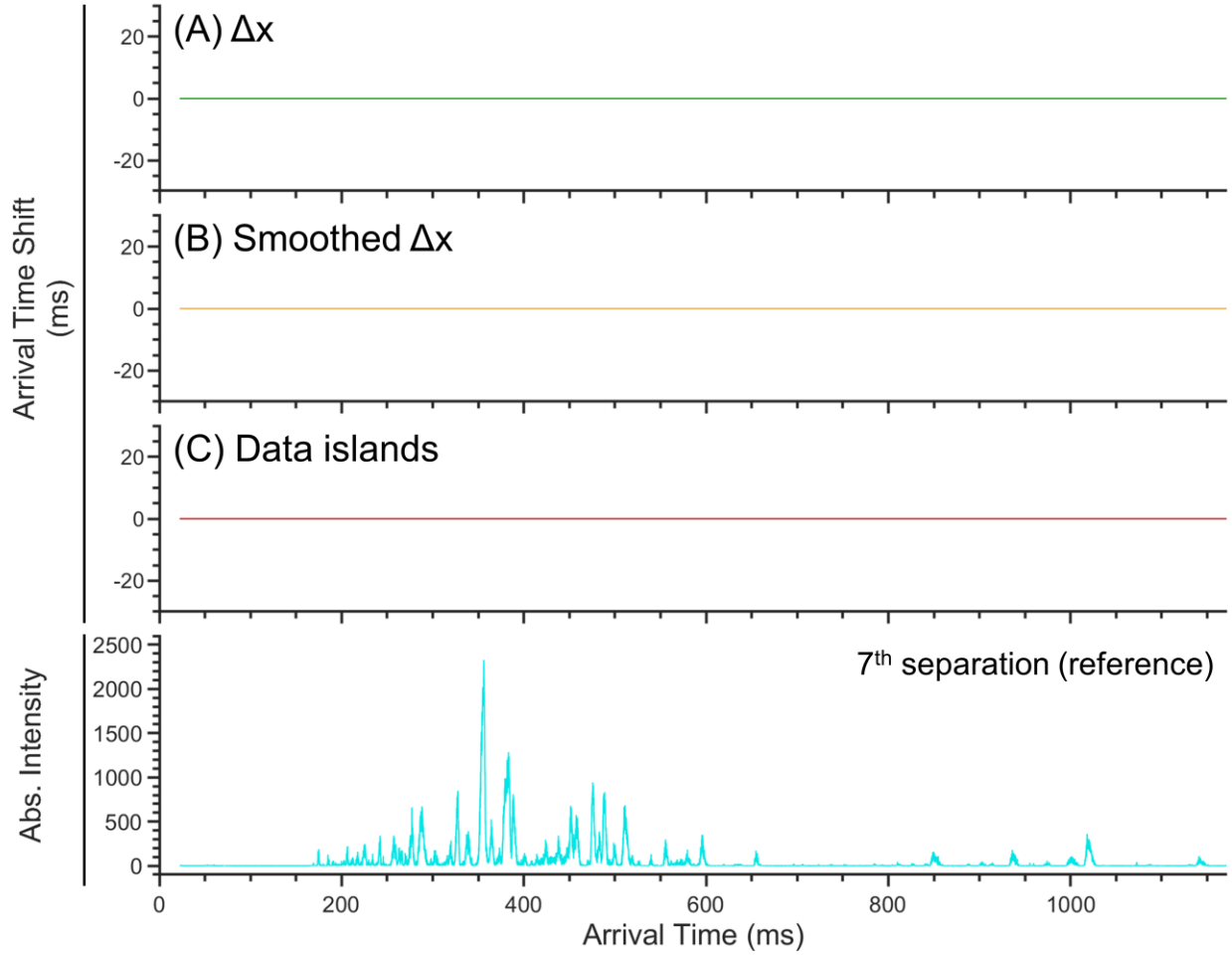

Figure S11: Dynamic time warping process applied to the **7th separation** of ions in a phosphopeptide mixture out of 100 total separations. (A) Arrival time shifts, (B) smoothed arrival time shifts, and (C) arrival time shifts after identifying data islands.

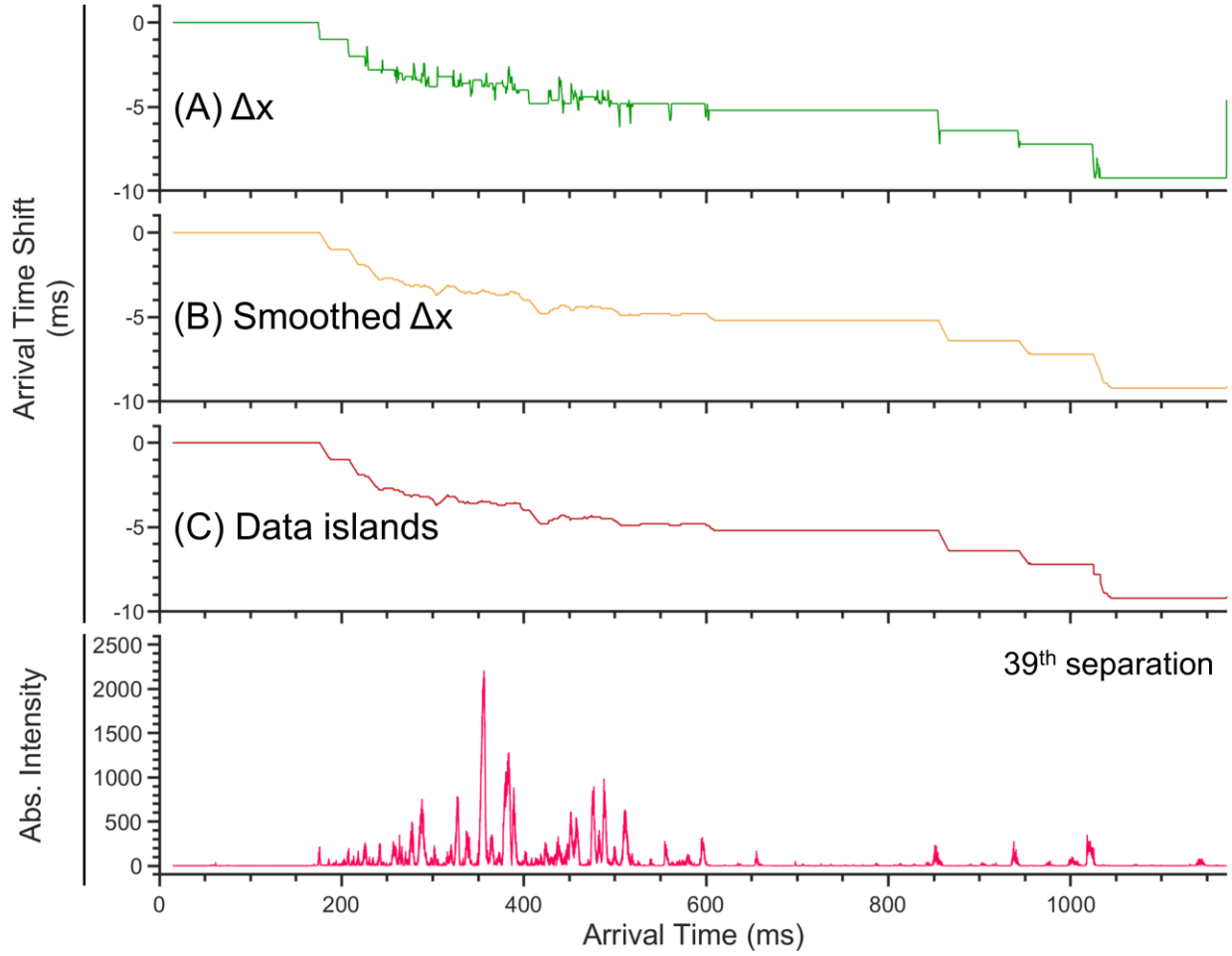

Figure S12: Dynamic time warping process applied to the **39th separation** of ions in a phosphopeptide mixture out of 100 total separations. (A) Arrival time shifts, (B) smoothed arrival time shifts, and (C) arrival time shifts after identifying data islands.

Description of isomer separation using DTW

The phosphopeptide mixture used here contained three sets of isomers, two per set (TPSSEEISPTK, SSSPELVTHLK, TPSSEEISPTKFPGLYR) due to phosphorylation at different serine residues. Extracted ion mobility spectra for the 2+ charge state of each isomeric set are shown in Figure S13. These data were acquired using only one SLIM level, whereas previous mobility spectra were acquired using four levels. The first set of isomers to traverse the single SLIM level corresponded to $TPSSEEISPTK^{2+}$ (Figure S13A). The isomers were partially resolved and a small hump was present on the tailing edge of the peak. The resolution between the $TPSSEEISPTK^{2+}$ isomers slightly improved when the data was subject to SVA (Figure S13B). However, the peak shape did not change when DTW was employed (Figure S13C). Partially resolved isomers will not merge because they will be identified as a single peak island and shifted by the same offset. The second set of isomers to traverse the SLIM corresponded to $SSSPELVTHLK^{2+}$, which were also partially resolved (Figure S13D). A small increase in resolution was obtained when the SVA aligner was used (Figure S13E), but again, no peak merging occurred when DTW was used (Figure S13F). The third set of isomers corresponded to $TPSSEEISPTKFPGLYR^{2+}$. Unlike the previous two isomeric sets, the third set of isomers were low intensity but well resolved (Figure S13G). After SVA, a small resolution improvement was obtained for the higher intensity isomer, but no noticeable effect occurred for the lower intensity isomer (Figure S13H). Additionally, there was no easily discernable difference between the SVA aligned and DTW aligned mobility spectra (Figure S13I). This once again illustrates that DTW does not merge isomers.

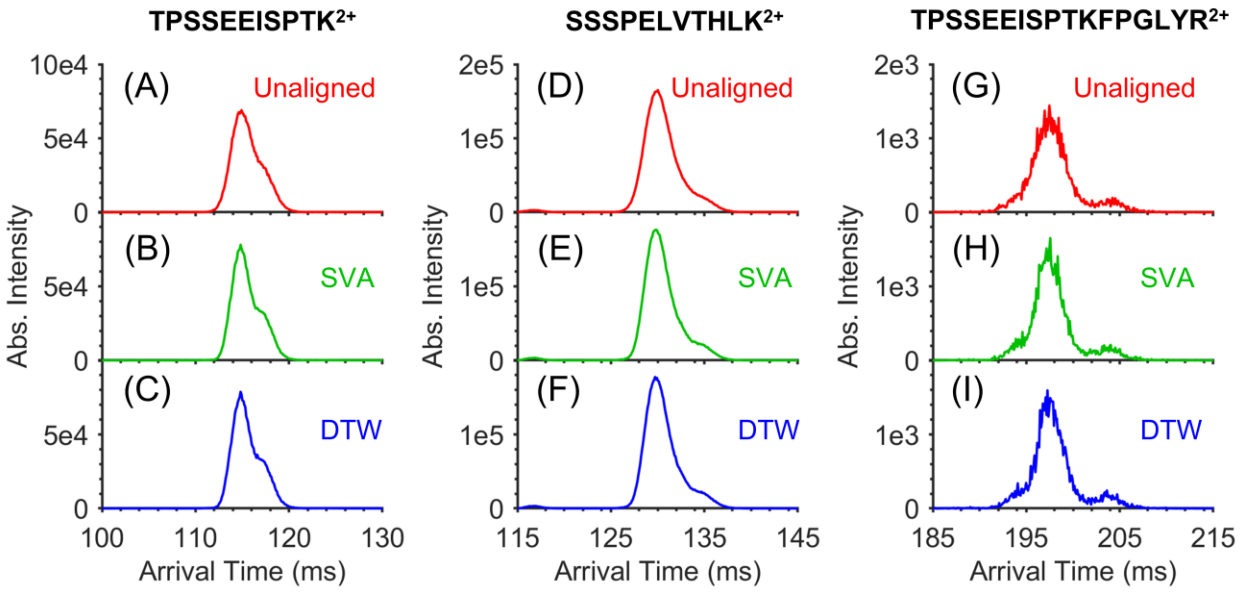

Figure S13: Effects of SVA and DTW on the resolution of phosphopeptide isomers in a phosphopeptide mixture using one ion level of the multilevel SLIM IMS. The data shows that DTW does not combine isomer peaks (i.e. monotonicity constraint).

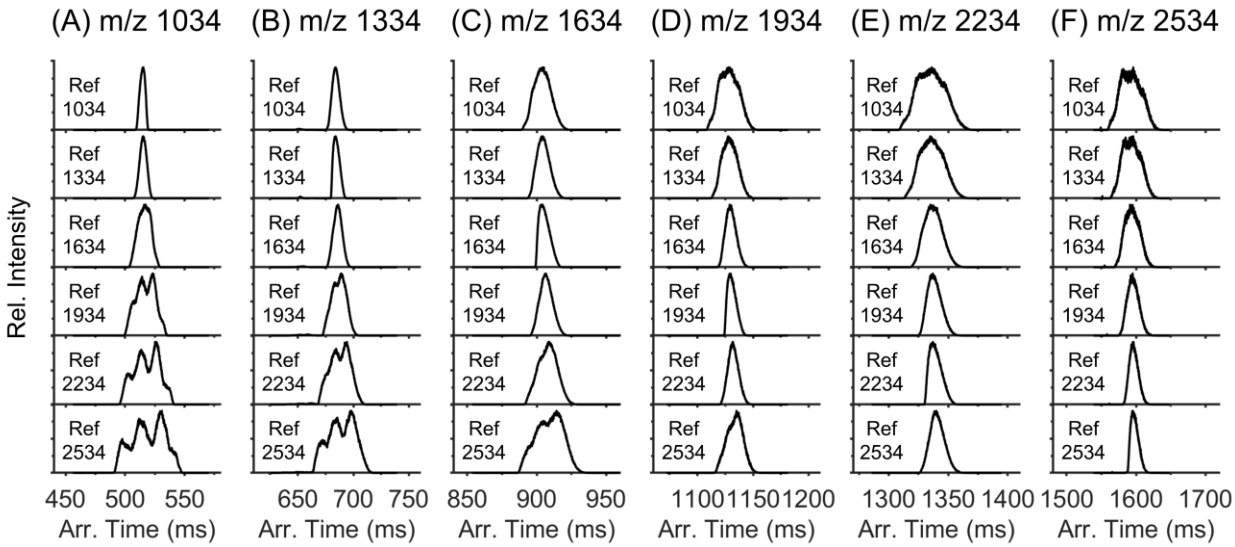

Figure S14: Effect of SVA aligner on peak shapes when using different negative Agilent tuning mixture ions as the reference peak.

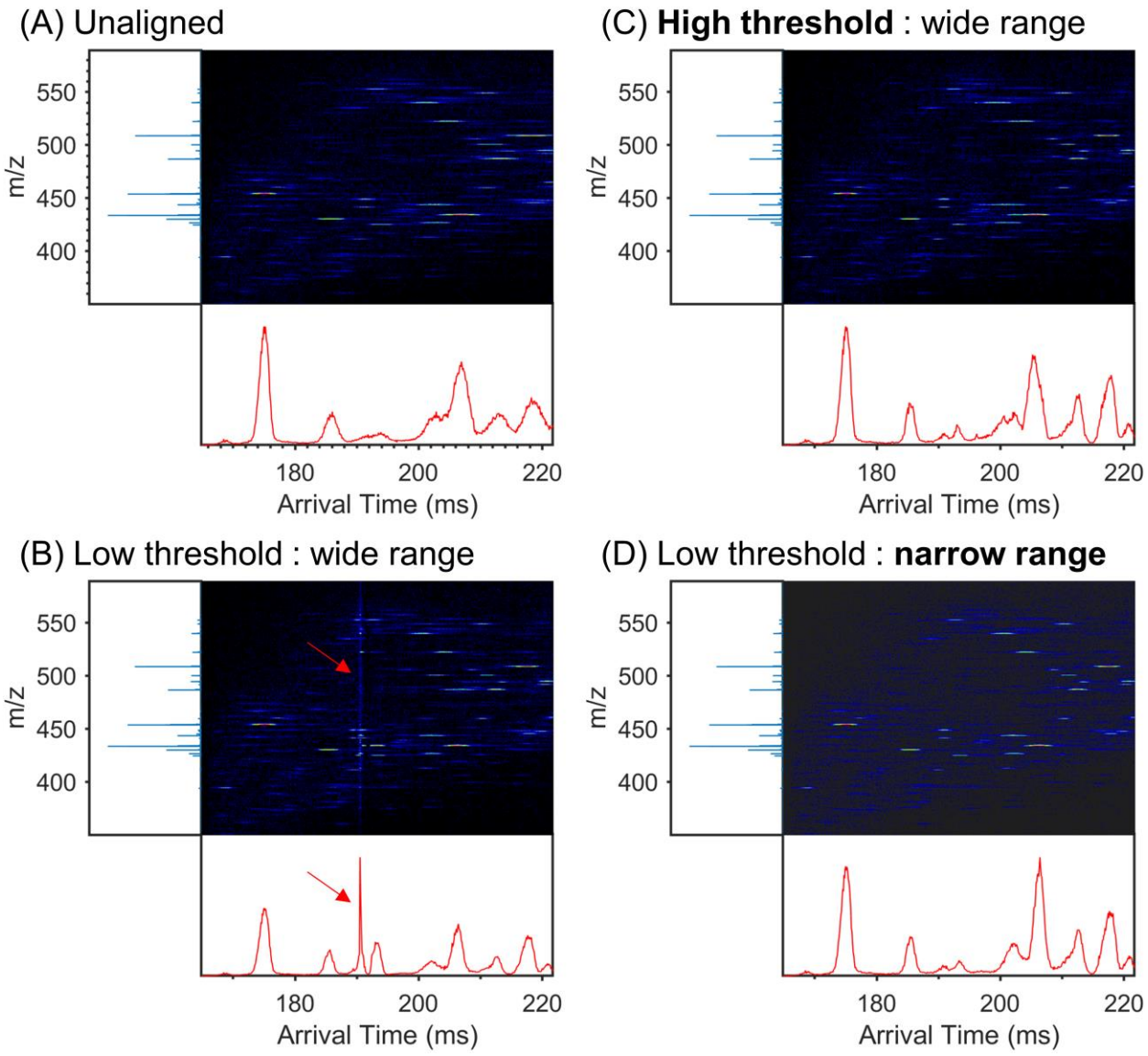

Figure S15: (A) Unaligned mobility spectrum of high mobility ions from a phosphopeptide mixture. (B) DTW aligned mobility spectrum showing an alignment artifact caused by the use of a low intensity threshold and a wide of a constraining range. (C) DTW aligned mobility spectrum showing no artifact due to the use of a higher intensity threshold. (D) DTW aligned mobility spectrum showing no artifact due to the use of a narrow constraining range. Sum = 100 frames.

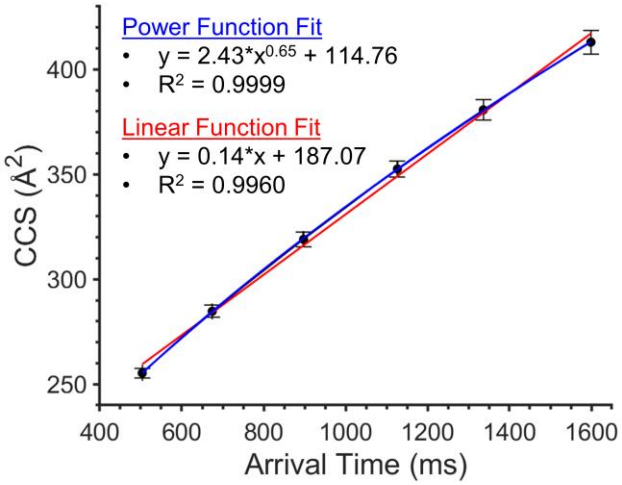

Figure S16: Power (blue) and linear (red) function fits to a plot of CCS vs arrival times of negative Agilent tuning mixture ions (m/z 1034, 1334, 1634, 1934, 2234, 2534). CCS values and errors were obtained from Stow et al.[2] Arrival times of ions were extracted from Figure 1.

References

(1) Hollerbach, A. L.; Li, A.; Prabhakaran, A.; Nagy, G.; Harrilal, C. P.; Conant, C. R.; Norheim, R. V.; Schimelfenig, C. E.; Anderson, G. A.; Garimella, S. V. B.; Smith, R. D.; Ibrahim, Y. M. Ultra-High-Resolution Ion Mobility Separations Over Extended Path Lengths and Mobility Ranges Achieved using a Multilevel Structures for Lossless Ion Manipulations Module, *Anal. Chem.* **2020**, *92*, 7972-7979.
(2) Stow, S. M.; Causon, T. J.; Zheng, X.; Kurulugama, R. T.; Mairinger, T.; May, J. C.; Rennie, E. E.; Baker, E. S.; Smith, R. D.; McLean, J. A.; Hann, S.; Fjeldsted, J. C. An Interlaboratory Evaluation of Drift Tube Ion Mobility–Mass Spectrometry Collision Cross Section Measurements, *Anal. Chem.* **2017**, *89*, 9048-9055.